

Ordering-induced band-gap reduction in $\text{InAs}_{1-x}\text{Sb}_x$ ($x \approx 0.4$) alloys and superlattices

S. R. Kurtz, L. R. Dawson, R. M. Biefeld, D. M. Follstaedt, and B. L. Doyle

Sandia National Laboratories, Albuquerque, New Mexico 87185

(Received 3 March 1992)

Ordering on the $\{111\}$ planes of the group-V sublattice (CuPt type) is demonstrated in molecular-beam-epitaxy grown $\text{InAs}_{1-x}\text{Sb}_x$ ($x \approx 0.4$) alloys and strained-layer superlattices (SLS's) using transmission electron diffraction. Accompanying ordering, a significant reduction of the band gap of the alloy was observed through infrared photoluminescence and photoconductive response measurements. An ordered SLS displayed a photoresponse at longer wavelength than the ordered alloy, due to a type-II band offset of the ordered constituents of the SLS. The band-gap reduction caused by ordering in these samples indicates that $\text{InAs}_{1-x}\text{Sb}_x$ alloys can effectively span the 8–12- μm atmospheric window for long-wavelength, infrared-detector applications.

There is considerable interest in $\text{InAs}_{1-x}\text{Sb}_x$ alloys and heterostructures for (III-V)-based, long-wavelength detectors and sources. With a type-II (or staggered) band offset, $\text{InAs}_{1-x}\text{Sb}_x$ strained-layer superlattices (SLS's) have displayed photoresponses at wavelengths $> 10 \mu\text{m}$,^{1,2} and prototype long-wavelength infrared (LWIR) photodiodes have been constructed.³ However, the minimum band gap reported for $\text{InAs}_{1-x}\text{Sb}_x$ alloys grown by molecular-beam epitaxy⁴ (MBE) is 145 meV (8.6 μm), observed in $\text{InAs}_{0.37}\text{Sb}_{0.63}$ at low temperature. The band gaps of disordered $\text{InAs}_{1-x}\text{Sb}_x$ alloy samples grown by zone recrystallization⁵ were in close agreement with those observed in recent MBE samples. Based on previous work, intrinsic $\text{InAs}_{1-x}\text{Sb}_x$ alloys appeared unable to span the 8–12 μm atmospheric window for LWIR detector applications.

Recently, compositional ordering on the $\{111\}$ planes has been observed in a number of III-V ternary systems,^{6–12} including $\text{InAs}_{1-x}\text{Sb}_x$.^{9,10} Pseudopotential calculations for completely ordered ternaries with 50%–50% compositions indicate that a significant reduction of the direct band gap will result, and a semimetal may occur for completely ordered $\text{InAs}_{0.5}\text{Sb}_{0.5}$.¹³ Previously, there has been no report of the optical properties of ordered $\text{InAs}_{1-x}\text{Sb}_x$ materials. In this paper we determine the band gap of an ordered $\text{InAs}_{1-x}\text{Sb}_x$ ($x \approx 0.4$) alloy and SLS using infrared photoluminescence and photoconductive response measurements. Significant band-gap reduction is observed for these samples, and this initial study demonstrates that ordered $\text{InAs}_{1-x}\text{Sb}_x$ alloys need to be reexamined for device applications requiring high speed or long-wavelength photoresponse.

$\text{InAs}_{1-x}\text{Sb}_x$ samples were grown using MBE. For the $\text{InAs}_{1-x}\text{Sb}_x$ material, the growth temperature was 425°C, and the growth rate was 1 $\mu\text{m}/\text{h}$. The growth temperature used in this study was lower than that reported in other MBE studies of $\text{InAs}_{1-x}\text{Sb}_x$ alloys,⁴ thus promoting ordering. Elemental sources were used to produce the In and Sb_4 beams. As_2 was generated by thermal cracking at 900°C. A total group-V:group-III equivalent pressure ratio of ≈ 3.0 was used for $\text{InAs}_{1-x}\text{Sb}_x$ growth. Sample quality must be maintained in order to observe photoluminescence and sharp absorption edges. To re-

duce dislocations resulting from lattice mismatch of the $\text{InAs}_{1-x}\text{Sb}_x$ with the substrate, a strain-relief buffer consisting of an $\text{Al}_{0.7}\text{In}_{0.3}\text{Sb}/\text{AlSb}$ SLS with graded layer thicknesses was grown on top of a (001) GaSb substrate. The Al alloy buffer was grown at 550°C. Compositions for the alloy and SLS samples were determined from double-crystal x-ray rocking curve measurements. The composition of the alloy was found to be $\text{InAs}_{0.60}\text{Sb}_{0.40}$ (± 0.01 uncertainty in composition). For the $\text{InAs}_{1-x}\text{Sb}_x$ SLS sample, position sensitive 2θ detection¹⁴ was also used to distinguish more clearly the $\text{InAs}_{1-x}\text{Sb}_x$ SLS x-ray peaks from those of the underlying $\text{AlInSb}/\text{AlSb}$ strain relief buffer. The composition of the SLS was found to be $\text{InAs}_{0.62}\text{Sb}_{0.38}/\text{InAs}_{0.54}\text{Sb}_{0.46}$ (± 0.01 uncertainty in compositions) with equal layer thicknesses of $83 \pm 5 \text{ \AA}$. The $\text{InAs}_{1-x}\text{Sb}_x$ material was 4 μm thick for both the alloy and SLS samples to insure that the infrared luminescence and photoresponse originates solely from the narrow band-gap material.

Cross-sectional specimens for transmission electron microscopy (TEM) were prepared by cleaving along (110), mechanically thinning, and ion milling the $\text{InAs}_{1-x}\text{Sb}_x/\text{InSb}$ materials. The specimens were examined in a $\langle 110 \rangle$ direction perpendicular to the [001] growth direction. Transmission electron diffraction (TED) and TEM images were obtained with a Phillips CM20ST (200 keV) microscope. Only one of the two $\langle 110 \rangle$ cross-sectional directions was examined in each material; the exact orientations of the cross sections were not determined.

Figure 1 shows the TED pattern for the $\text{InAs}_{0.60}\text{Sb}_{0.40}$ alloy, and Fig. 2 is the pattern for the SLS. Relevant zinc-blende reflections have been indexed on the photographs. Both specimens show additional, non-zinc-blende, weak reflections at half the distance between (000) and $\{111\}$ spots as indicated by arrows. These weak reflections indicate that CuPt-type ordering is taking place. Indices in Figs. 1 and 2 are assigned based on the assumption that only two of the four $\langle 111 \rangle$ variants are present. The $\langle 111 \rangle$ variants assumed to be present are those reported for $\text{InAs}_{1-x}\text{Sb}_x$ grown by metal-organic chemical vapor deposition and found in a large number of III-V ternary materials.^{6–12} The two sets of spots indicate that two variants of the ordered structure are present in separate

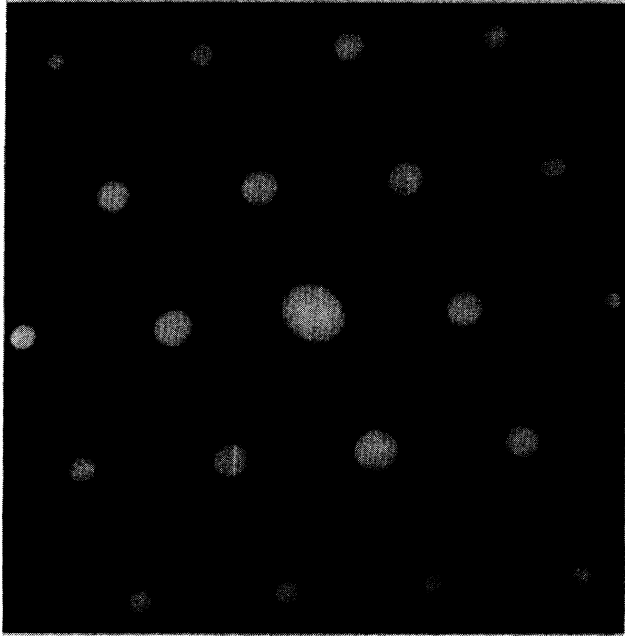


FIG. 1. Transmission electron-diffraction pattern from a $\langle 110 \rangle$ cross section of an $\text{InAs}_{0.6}\text{Sb}_{0.4}$ alloy grown by MBE on (001)-oriented GaSb. Reflections due to CuPt-like ordering are indicated by arrows.

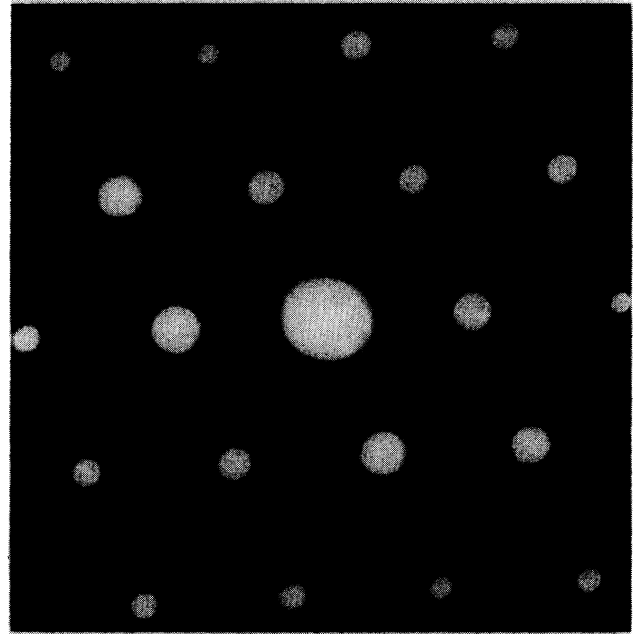


FIG. 2. Transmission electron-diffraction pattern from a $\langle 110 \rangle$ cross section of an $\text{InAs}_{0.62}\text{Sb}_{0.38}/\text{InAs}_{0.54}\text{Sb}_{0.46}$ strained-layer superlattice grown by MBE on (001)-oriented GaSb. Reflections due to CuPt-like ordering are indicated by arrows.

domains. In the SLS two variants were clearly resolvable. In the alloy, however, the ordering reflections along $(1\bar{1}1)$ are sharper and more intense than the faint reflections along $(\bar{1}11)$. The latter variant of the alloy and both variants of the SLS are elongated in a direction tilted off the $\langle 001 \rangle$ growth axis toward their respective ordering axes. These elongated reflections are like those found for $\text{GaAs}_{0.5}\text{Sb}_{0.5}$ grown at lower temperatures where the CuPt-type ordering is not well developed.¹⁰ This elongation has been shown to be due to the presence of platelike domains.¹¹ The difference in intensity of the two sets of spots in these samples indicates that one of the variants is preferred. Both materials exhibit faint streaks passing through the ordered reflections along the $\langle 001 \rangle$ growth direction. This streaking is similar to the streaking reported for InGaP.⁸ In the alloy (Fig. 1), low intensity streaks can be seen in the $\langle 111 \rangle$ directions through the zinc-blende spots due to the faulting observed in images of the material. Additional weak reflections are also detected at approximately $\frac{1}{4}$ and $\frac{3}{4}$ of the distance to the (002) spot; their meaning is not yet understood. Direct imaging of the superlattice with TEM indicated a periodicity of 156 Å, in reasonable agreement with the 166 Å obtained from the x-ray measurement.

Infrared photoluminescence was measured using a double modulation experiment with CO laser pump.² Photoluminescence spectra for the $\text{InAs}_{0.60}\text{Sb}_{0.40}$ alloy sample are shown in Fig. 3(a). The photoluminescence intensity was proportional to laser power except at the highest pump power where the intensity saturates and heating is occurring as evidenced by increased linewidth and a shift to higher energy. Characteristic of interband luminescence, the high-energy edge of the photoluminescence in-

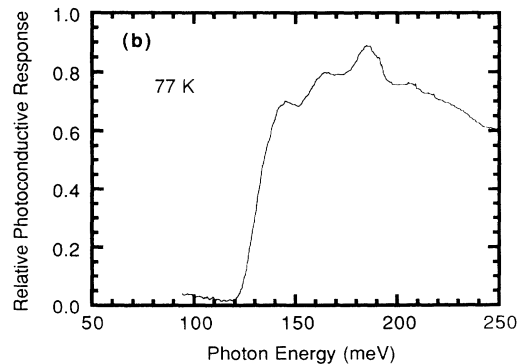
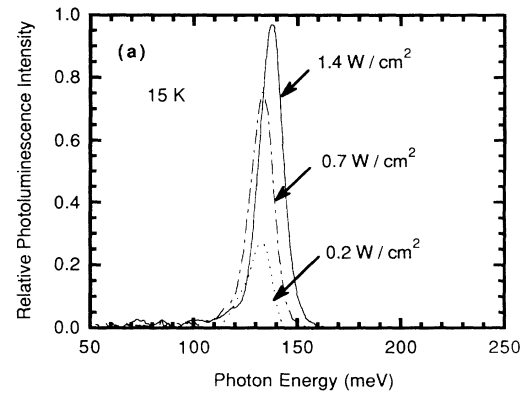


FIG. 3. (a) Infrared photoluminescence spectra for $\text{InAs}_{0.60}\text{Sb}_{0.40}$ alloy obtained with optical pump powers as indicated. Sample temperature is 15 K. (b) Photoconductive response spectrum for an $\text{InAs}_{0.60}\text{Sb}_{0.40}$ alloy at 77 K.

tensity can be described by

$$I(\hbar\omega) \propto \omega^2(\hbar\omega - E_{\text{gap}})^{1/2} \exp[-(\hbar\omega - E_{\text{gap}})/kT_e], \quad (1)$$

where T_e is an effective temperature.¹⁵ At the lowest pump power shown in Fig. 3(a), T_e approaches the sample temperature. ($T_e = 30$ K compared to a sample temperature of 15 K.) Surprisingly, the photoluminescence was dominated by a single, narrow peak over a wide range of pump power and temperature. Domains of ordered and disordered alloy should lead to significant line-shape distortion or multiple peaks, and these observations suggest that the sample is homogeneous in composition and degree of ordering when averaged over a minority carrier diffusion length.

Ti/Au contacts were deposited on the surface of the $\text{InAs}_{0.60}\text{Sb}_{0.40}$ alloy, and the photoconductive response was measured [Fig. 3(b)]. This spectrum is dominated by a single, sharp, low-energy band-edge feature occurring at the same energy as the peak in the photoluminescence spectra at low power (132 meV). In addition to the band edge, oscillations are observed in the photoresponse with a period (22 meV) equal to the optical-phonon energy observed from phonon-assisted recombination in InSb .¹⁵ Infrared transmission studies were not performed due to free carrier absorption in the available GaSb substrates.

Compared with the band gap of previously reported $\text{InAs}_{1-x}\text{Sb}_x$ alloys, the band gap of the ordered $\text{InAs}_{0.60}\text{Sb}_{0.40}$ alloy is shifted to significantly lower energy. Using the energy of the photoluminescence peak,⁴ we obtain a band gap of 132 meV (9.4 μm) for the ordered alloy. Previous studies of $\text{InAs}_{1-x}\text{Sb}_x$ alloys predict a band gap of 177 meV (7.0 μm) for $\text{InAs}_{0.60}\text{Sb}_{0.40}$ at low temperature. This value has been determined from self-consistent absorption and photoluminescence data on samples spanning the entire range of $\text{InAs}_{1-x}\text{Sb}_x$ ternary compositions.^{4,5} Also, an $\text{InAs}_{0.6}\text{Sb}_{0.4}$ photodiode displayed a cutoff wavelength of 7.0 μm .¹⁶ Ordering has reduced the band gap of the $\text{InAs}_{0.60}\text{Sb}_{0.40}$ alloy by 45 meV, and ordered $\text{InAs}_{1-x}\text{Sb}_x$ ($x \approx 0.5$ – 0.6) should achieve even longer wavelengths. We are optimistic that the growth conditions of $\text{InAs}_{1-x}\text{Sb}_x$ may be optimized to enhance ordering and resulting band-gap narrowing.

Photoluminescence and photoconductive response spectra for the $\text{InAs}_{0.62}\text{Sb}_{0.38}/\text{InAs}_{0.54}\text{Sb}_{0.46}$ SLS are shown in Fig. 4. The photoluminescence peak and the band edge in the photoresponse are in excellent agreement, and an SLS band gap of 117 meV (10.6 μm) is observed. The SLS photoresponse is approximately 80 meV lower in energy than the value predicted from accepted band gaps in $\text{InAs}_{1-x}\text{Sb}_x$ ternaries and band offsets measured in Sb-rich, $\text{InAs}_{1-x}\text{Sb}_x$ SLS's.² Obviously, the band-gap decrease of the ordered $\text{InAs}_{1-x}\text{Sb}_x$ constituents of the SLS is extending the photoresponse of the SLS to longer wavelength. Distinct oscillations with a period of 36 meV are observed in the SLS photoconductive response.

We believe that the ordered SLS has a type-II band offset of the same magnitude as that observed in Sb-rich SLS's. Using 132 meV for the band gap of the ordered alloy constituents and a type-II, unstrained valence band offset of 29 meV, we calculate a quantum-size shifted

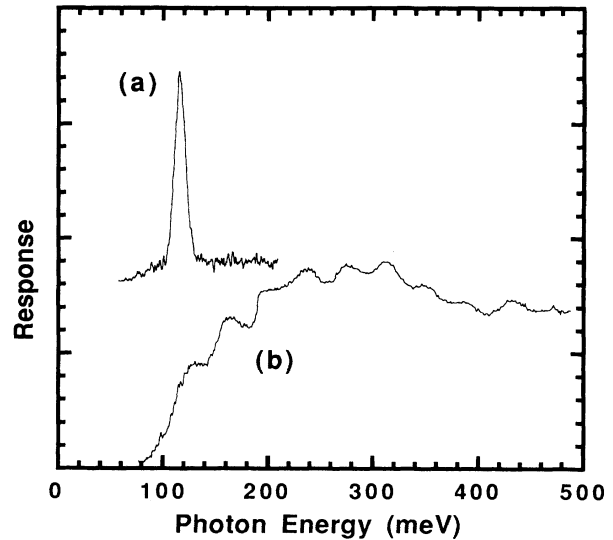


FIG. 4. (a) Photoluminescence spectrum (15 K) of an $\text{InAs}_{0.62}\text{Sb}_{0.38}/\text{InAs}_{0.54}\text{Sb}_{0.46}$ (83 Å/83 Å layer thicknesses) SLS. The laser pump intensity was 0.6 W/cm^2 . (b) Spectral response (77 K) of a photoconductive detector fabricated from this SLS.

band gap of 119 meV for the ordered $\text{InAs}_{0.62}\text{Sb}_{0.38}/\text{InAs}_{0.54}\text{Sb}_{0.46}$ SLS.² In making this estimate, the alloy and SLS samples are both assumed to be ordered to the same degree. Phonon-assisted photoconductivity produces oscillations like those observed in our spectra with a period

$$\Delta E = \hbar\omega_{\text{LO}}(1 + m_e/m_h), \quad (2)$$

where $\hbar\omega_{\text{LO}}$ is an LO phonon energy, and m_e and m_h are electron and hole effective masses, respectively.¹⁷ In the alloy sample where the light- and heavy-hole bands are nearly degenerate, m_h is a heavy-hole mass, and the period of oscillation is approximately the LO phonon energy. The larger period of the oscillation observed in the SLS spectra is consistent with a type-II offset. With a type-II offset, the hole quantum well is located in the bi-axially compressed $\text{InAs}_{0.54}\text{Sb}_{0.46}$ layer of the SLS. The hole ground state in this layer is "lightlike," reducing m_h and increasing the oscillation period. From the SLS oscillation period, we find a m_e/m_h ratio of approximately 0.6. This value is consistent with masses observed in Sb-rich, type-II $\text{InAs}_{1-x}\text{Sb}_x$ SLS's.^{2,18}

As a result of ordering, significant reduction in the band gap of $\text{InAs}_{1-x}\text{Sb}_x$ ($x \approx 0.4$) alloys and SLS's has been demonstrated. Although the "perfect" ordering envisioned in band-structure calculations¹³ has probably not been achieved, we believe that this study is an indication of the material properties that can be obtained under MBE growth conditions producing device-quality $\text{InAs}_{1-x}\text{Sb}_x$ films. The band-gap reduction observed in these samples indicates that $\text{InAs}_{1-x}\text{Sb}_x$ alloys can effectively span the 8–12- μm window for LWIR detector applications. As needed, further band-gap reduction can be obtained with ordered $\text{InAs}_{1-x}\text{Sb}_x$ SLS's. We present evidence that a type-II band offset occurs in these As-rich SLS's.

We thank our colleagues, J. S. Nelson, C. R. Hills, and J. R. Reno, for useful discussions. J. R. Hubbs and D. B. Webb provided technical assistance. This work was performed at Sandia National Laboratories, supported by the U.S. Department of Energy under Contract No. DE-AC04-76DP00789.

-
- ¹S. R. Kurtz, G. C. Osbourn, R. M. Biefeld, L. R. Dawson, and H. J. Stein, *Appl. Phys. Lett.* **52**, 831 (1988).
- ²S. R. Kurtz and R. M. Biefeld, *Phys. Rev. B* **44**, 1143 (1991).
- ³S. R. Kurtz, L. R. Dawson, T. E. Zipperian, and R. D. Whaley, Jr., *IEEE Electron. Devices Lett.* **11**, 54 (1990).
- ⁴M. Y. Yen, R. People, K. W. Wecht, and A. Y. Cho, *Appl. Phys. Lett.* **52**, 489 (1988).
- ⁵W. M. Coderre and J. C. Woolley, *Can. J. Phys.* **46**, 1207 (1968).
- ⁶G. B. Stringfellow, *J. Cryst. Growth* **98**, 108 (1989).
- ⁷G. B. Stringfellow and G. S. Chen, *J. Vac. Sci. Technol. B* **9**, 2182 (1991).
- ⁸A. Gomyo, T. Suzuki, and S. Iijima, *Phys. Rev. Lett.* **60**, 2645 (1988).
- ⁹J. R. Yen, K. Y. Ma, and G. B. Stringfellow, *Appl. Phys. Lett.* **54**, 1154 (1989).
- ¹⁰Y.-E. Ihm, N. Otsuka, J. Klem, and H. Morkoc, *Appl. Phys. Lett.* **51**, 2013 (1987).
- ¹¹P. Bellon, J. P. Chevalier, G. P. Martin, E. Dupont-Nivet, C. Thiebaut, and J. P. Andre, *Appl. Phys. Lett.* **52**, 567 (1988).
- ¹²G. S. Chen, T. Y. Wang, and G. B. Stringfellow, *Appl. Phys. Lett.* **56**, 1463 (1990).
- ¹³Su-Huai Wei and Alex Zunger, *Appl. Phys. Lett.* **58**, 2684 (1991).
- ¹⁴S. T. Picraux, B. L. Doyle, and J. Y. Tsao, *Semiconductors and Semimetals*, edited by T. P. Pearsall (Academic, New York, 1991), Vol. 33, p. 139.
- ¹⁵A. Mooradian and H. Y. Fan, *Phys. Rev.* **148**, 873 (1966).
- ¹⁶D. T. Cheung, A. M. Andrews, E. R. Gertner, G. M. Williams, J. E. Clarke, J. G. Pesko, and J. T. Longo, *Appl. Phys. Lett.* **30**, 587 (1977).
- ¹⁷Roger W. Shaw, *Phys. Rev. B* **3**, 3283 (1971).
- ¹⁸S. Y. Lin, D. C. Tsui, L. R. Dawson, C. P. Tigges, and J. E. Schirber, *Appl. Phys. Lett.* **57**, 1015 (1990).

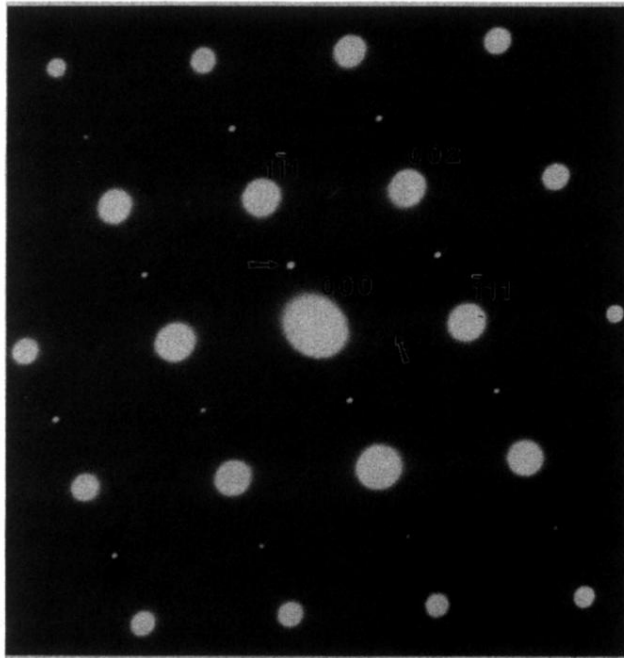


FIG. 1. Transmission electron-diffraction pattern from a $\langle 110 \rangle$ cross section of an $\text{InAs}_{0.6}\text{Sb}_{0.4}$ alloy grown by MBE on (001) -oriented GaSb. Reflections due to CuPt-like ordering are indicated by arrows.

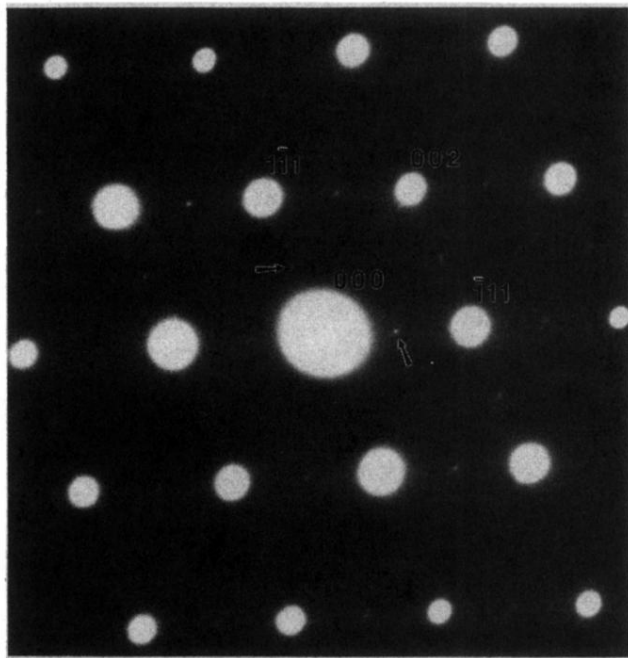


FIG 2. Transmission electron-diffraction pattern from a $\langle 110 \rangle$ cross section of an $\text{InAs}_{0.62}\text{Sb}_{0.38}/\text{InAs}_{0.54}\text{Sb}_{0.46}$ strained-layer superlattice grown by MBE on (001)-oriented GaSb. Reflections due to CuPt-like ordering are indicated by arrows.